

Nanoscale

Accepted Manuscript



This is an *Accepted Manuscript*, which has been through the Royal Society of Chemistry peer review process and has been accepted for publication.

Accepted Manuscripts are published online shortly after acceptance, before technical editing, formatting and proof reading. Using this free service, authors can make their results available to the community, in citable form, before we publish the edited article. We will replace this *Accepted Manuscript* with the edited and formatted *Advance Article* as soon as it is available.

You can find more information about *Accepted Manuscripts* in the [Information for Authors](#).

Please note that technical editing may introduce minor changes to the text and/or graphics, which may alter content. The journal's standard [Terms & Conditions](#) and the [Ethical guidelines](#) still apply. In no event shall the Royal Society of Chemistry be held responsible for any errors or omissions in this *Accepted Manuscript* or any consequences arising from the use of any information it contains.

**Improving energy conversion efficiency for triboelectric nanogenerator with
capacitor structure by maximizing surface charge density**

Xianming He, Hengyu Guo, Xule Yue, Jun Gao, Yi Xi, Chenguo Hu *

X. M. He, H. Y. Guo, X. L. Yue, Dr. Y. Xi, Prof. C. G. Hu

Department of Applied Physics, Chongqing University Chongqing 400044, PR China

E-mail: hucg@cqu.edu.cn (C. G. Hu)

J. Gao

Chongqing Univ, State Key Lab Power Transmiss Equipment & Syst Se, Chongqing

400044, PR China

Abstract

Nanogenerators with the capacitor structure based on piezoelectricity, pyroelectricity, triboelectricity and electrostatic induction have been extensively investigated. Although the electron flow on electrodes is well understood, the maximum efficiency-dependent structure design is not clearly known. In this paper, a clear understanding of triboelectric generators with capacitor structure is presented by the investigation of polydimethylsiloxane-based composite film nanogenerators, indicating that the generator factually acts as an energy storage and output device. Maximum energy storage and output depend on the maximum charge density on dielectric polymer surface, which is determined by the capacitance of the device. The effective thickness of polydimethylsiloxane can be greatly reduced by mixing a suitable amount of conductive nanoparticles into the polymer, through which the charge density on the polymer surface can be greatly increased. This finding can be applied to all the triboelectric nanogenerators with capacitor structure and provides an important guide to the structure design for nanogenerators. It is demonstrated that graphite particles with size of 20-40 nm and 3.0% mass mixed into the polydimethylsiloxane can reduce 34.68% of the effective thickness of the dielectric film and increase the surface charges by 111.27% on the dielectric film. The output power density of the triboelectric nanogenerator with the composite polydimethylsiloxane film is 3.7 W/m^2 , which is 2.6 times as much as that of the pure polydimethylsiloxane film.

1. Introduction

Nanogenerators (NGs) based on piezoelectricity,¹⁻⁵ pyroelectricity,^{6,7} triboelectricity⁸⁻¹⁴ and electrostatic induction^{15,16} have been extensively investigated and they have presented a rapid progress in structure design for actual applications. Polydimethylsiloxane (PDMS) as a polymer electret has advantages of being flexible, transparent, biocompatible, non-toxic and cost effective and has been extensively used for flexible nanogenerators,^{17,18} nanodevices¹⁹ and nanosensors.^{20,21} In addition, PDMS can be easily made into composite films by mixing nanoparticles or other nanostructures^{22,23} or patterned on the surface or inner.²⁴ Nanocomposite piezoelectric generators based on PDMS with mixture of ZnO²² or BaTiO₃^{17,23} have been reported, which reveals that the output power is improved when compared with that of the pure PDMS. Meanwhile, if PDMS is mixed with co-mixture of ZnO and carbon nanotubes²⁵ or BaTiO₃ and graphite carbon,²⁶ the generator achieves higher output power. As we know that the dielectricity of PDMS separator is very important for a nanogenerator with a capacitor structure, then, what is the role of the carbon nanostructures in the polymer? Recently, spongy structure PVDF and PDMS based NGs have been found to possess better output power compared with the flat film based NGs.^{27,28} S-W Kim et al. propose that a sponge structured film possesses a thinner thickness than a flat film, which increases the relative capacitance by the increase in the effective (ϵ/d) value.²⁸ To find out how the effective ϵ/d value affects the output power of NGs and whether there is a relationship between the effective ϵ/d value and mixture of nanomaterials, we think it is necessary to investigate the role of a conductive

nanomaterial mixed into PDMS film in NG.

In this paper, we design and fabricate PDMS-based composite film nanogenerators (CFNG) by mixing PDMS with graphite particles (GPs). The output current, voltage and power are investigated systematically by mixing PDMS with a carbon material in different morphologies, particle sizes and contents, and by varying the CFNG structure in different film thicknesses and gaps between electrode and composite film, and under different measuring conditions. A clear understanding of triboelectric NG with the capacitor structure is presented, indicating that the generator factually acts as an energy storage and output device. The capacitance of the NG plays an important role in maximizing charge density on the polymer surface. Bigger ϵ/d value can achieve higher charge density on the polymer surface. The effective d value can be largely reduced by mixing PDMS with a suitable amount of conductive graphite nanoparticles with a little change of relative dielectric constant. This finding can be applied to all the triboelectric NGs with a capacitor structure and provides an important guide to the structure design for NGs. It is found that GPs with size of 20-30 nm and 3.0% ratio is the best to be mixed into PDMS, where the effective thickness d of the dielectric film can decrease 34.68% and surface charges on the dielectric film can increase 111.27%. After optimizing the thickness of the composite film and the gap between electrode and the composite film in the CFNG, the output power of 1.48 mW (3.7 W/m^2) is obtained, which can be used to light up 52 blue LEDs in series. The CFNG has good stability, durability and integratability. In addition, with the advantages of high output power and biocompatibility, the CFNG has wide application prospects in flexible sensors and

biological devices field.

2. Results and discussion

A schematic diagram of the fabrication process for PDMS mixed with GPs (PDMS@GPs) thin film and its composite film nanogenerator (CFNG) are shown in Fig. 1a. The fabrication process could be described as four steps, solution mixing → film forming → film cutting → CFNG preparation. More detailed steps can be found in the *experimental section*. The prepared composite film is cut into rectangles and assembled into the CFNG with Al foil electrodes and hardboard. Fig. 1b shows the digital photograph of PDMS@GPs thin film, which has excellent flexibility. The materials in the tubes in the inset A-E are pure PDMS, pure curing agent, GPs dispersed in alcohol, PDMS@GPs mixed in alcohol, curing agent@GPs dispersed in alcohol, respectively, indicating that after GPs are mixed into PDMS, the solution color changes from colorless to light black. The CFNG device has a sandwich-like structure in rectangular shape as is shown in Fig. 1c. The GPs are uniformly mixed into PDMS matrix and X-ray diffraction (XRD) patterns of PDMS@GPs thin film with different GP contents (0.0 g, 0.01 g, 0.05 g, 0.1 g) are shown in Fig. S1, which demonstrate a graphite structure (JCPDS No.75-2078) of GPs, and the intensity of the peaks increases with the increase in GP content.

2.1. Influence of GPs mixed into PDMS on CFNG

The CFNG has a sandwich-like structure with the PDMS@GPs thin film in the middle as is shown in Fig. 1a. It can be regarded as a flat-panel capacitor with an external load of R (Fig. 2a). To compare the performance of the composite PDMS

film with the pure PDMS film, the NGs using different conductive carbon composite films in the same film size (2×2 cm) and thickness are fabricated and measured. Fig. 2b shows the output current of the NGs using the pure PDMS film and composite PDMS films mixed with the same weight (0.1 g) of graphite particles, graphenes and carbon fibers, from which we can see that the output current is greatly enhanced after the PDMS are mixed with conductive carbon materials. Among them, the PDMS mixed with graphite particles has best performance and its output current of 16.5 μA is about 4.5, 1.6 and 2.3 times as much as that of the pure PDMS film, the PDMS film mixed with graphenes and carbon fibers, respectively. Photographs of the pure PDMS film and PDMS films mixed with the same weight of graphite particles, graphenes and carbon fiber are shown in Fig. 2c, indicating that the graphite particles have best dispersibility in the PDMS film.

To look into the influence of GP size, a comparative experiment is also carried out on the composite films mixed with the same GP weight of 0.08 g but different GP sizes (3-5 nm, 10-20 nm, 20-30 nm, 30-40 nm, 80-100 nm), and the results are shown in Fig. 2d. From FE-SEM images of the GPs with different sizes in Fig. 2e we can see that all the particles are irregular. The output current of the film with GP sizes ranging from 20 nm to 40 nm is the highest. Smaller size (≤ 5 nm) might cause agglomeration of GPs in the PDMS film, while bigger size (≥ 80 nm) might not reach a suitable distribution in the PDMS film. To confirm the influence of GP concentration of the PDMS film on the CFNG, the PDMS@GPs films with different GP weights from 0.0 g to 1.0 g are fabricated. The output current of the CFNGs using composite films with

different GP weights (Fig. 3a) and mass percentages (Fig. 3b) in the same film size (2 cm × 2 cm) and thickness (0.45 mm) are measured at frequency of 2 Hz. The PDMS@GPs film with 0.1 g (3.0 wt%) GPs has maximum output current. The output current gradually increases from 3.0 μ A to 10.6 μ A when the GP content increases from 0.0 g to 0.1 g, however, it begins to decrease as the GP content is larger than 0.1 g. To find out the change of the dielectric property, the conductivity of the PDMS@GPs films with GP content from 0.0 g to 1.0 g is measured under different working frequencies (Fig. 3c). The conductivity has little change when the GP content is less than 0.3 g, demonstrating that they keep dielectricity well in this range of GP content. The digital photographs of the PDMS@GPs film with GP content from 0.0 g to 1.0 g are shown in Fig. 3d, indicating that the color is getting dark as the GP content increases. The measured relative dielectric constants of the composite films are listed in Table 1, which matches the conductivity results.

The output voltage, current and power of the CFNG with 0.1 g GPs, film size of 2×2 cm and thickness of 0.45 mm are measured with different external loads, as are shown in Fig. 4a. The output voltage achieves 286 V with a load resistance of 600 M Ω . The short current is about 26.8 μ A and the peak output power reaches 1.48 mW with a load resistance of 12 M Ω . Maximum output current and the partially enlarged view are shown in Fig. S2 and the CFNG can be used to light up at least 52 LEDs in series. Moreover, to prove its stability and durability, a test is carried out for 500 cycles (Fig. 4b), which shows little change in the output current. The output voltage, current and power of the CFNGs with the same film size and thickness and different

GP contents are displayed in Fig. S3. The internal resistance and the output power of the devices versus different GP contents are plotted in Fig. 4c, which indicates that the resistance decreases from 64.9 M Ω to 2.98 M Ω with an increase in GP content from 0.0 g to 0.1 g, and then it keeps almost a constant from 0.1 g to 0.2 g. The output power increases with an increase in GP content from 0.0 g to 0.1 g, but decreases rapidly afterwards, which indicates that the output power is not only determined by internal resistance due to the fact that it is a constant in GP content of 0.1-0.2 g. The open-circuit voltage of the CFNGs with different GP contents is shown in Fig. S4.

2.2. Optimization of size and structure of CFNG

To get a maximum power density, the structure size of CFNG has been optimized. The output current of the CFNG using the PDMS@GPs film (0.1 g GPs) with different aspect ratios (1 cm \times 2 cm, 2 cm \times 2 cm, 2 cm \times 3 cm, 1 cm \times 3 cm) are compared (Fig. 5a and b), from which we can see that the size of 2 cm \times 2 cm (aspect ratio 1:1) has the largest current density (4.4 μ A/cm²) due to the even pressure on the CFNG in this size. The output performance of the CFNG using the PDMS@GPs film with different thicknesses (0.15 mm, 0.30 mm, 0.45 mm, 0.60 mm, 0.75 mm) are measured (Fig. 5c and d). As can be seen that the output current is the largest with the film thickness of 0.45 mm. Compared the CFNG made by the PDMS@GPs film with the pure PDMS in thickness of 0.45 mm under the same conditions, the output current of the PDMS@GPs film device is about 7 times as large as that of the pure PDMS film device. Obviously, the PDMS mixed with 0.1 g GPs significantly improves the

output performance of CFNG. To further optimize the CFNG structure, the gap (n) between the upper electrode and the composite film is selected to be varied (0.2 mm, 0.5 mm, 0.8 mm) under different driving frequencies $f=2.0, 2.5, 3.0, 3.5, 4.0$ Hz. As is shown in Fig. 6a-d, the output current decreases with an increase in n and f , for the optimal working frequency of the CFNG is 2 Hz (Fig. S5) and the increase in n will result in the prolonged contacting/separating time of friction layers, which reduces the current according to the formula $I = dQ/dt$. However, too small gap n will block the separation of the friction layers. There should be a proper gap to achieve the best output performance of the CFNG.

2.3. Working mechanism of CFNG

The fundamental working mechanism is similar to that of the triboelectric NG based on the triboelectric and electrostatic induction effects.²⁹⁻³⁵ A schematic diagram of the CFNG working mechanism is shown in Fig. S6a and b. The output current corresponding to the pressing and releasing processes is also shown in Fig. S6c.

From the comparison of the performance of the PDMS@GPs film with the pure PDMS film in Fig. 2b, we can see that the output current is greatly enhanced by mixing the GPs into the PDMS film. To understand the role of GPs mixed in PDMS, we look into the structure of the CFNG. The CFNG can be regarded as a flat-panel capacitor with an external load of R as is shown in Fig. 7a, where ϵ_0 , ϵ_l , d and x represent the dielectric constant of the air, dielectric constant of the PDMS film, the thickness of the PDMS@GPs thin film and the thickness of the air layer, respectively. First, look at a NG made of pure PDMS film (Fig. 7a), as the negative charges on the

PDMS surface from the interface friction keeps constant due to its electret nature, two flat-panel capacitors should be included. One fixed capacitor consists of the bottom electrode and the surface of the electret film separated by a dielectric PDMS film with capacitance of $C_1 = \frac{\epsilon_1 S}{d}$ (S represents the friction area of PDMS film), and the other capacitor consists of the upper electrode and the surface of the electret film separated by a dielectric air with capacitance of $C_2 = \frac{\epsilon_0 S}{x}$, which will vary with the change in gap x . It is well known that a capacitor is a passive two-terminal electrical component used to store energy in an electric field. Capacitance of the capacitor is very important for the energy storage, which determines the maximum charge density on the surface of the electrodes. In our experiment, as the electric field is not electrostatic field, the charge densities on the upper and bottom electrodes are not constants, and charges transfer between them. But the charges on the surface of PDMS film cannot move. The capacitor structure affects directly the maximum charge density on the surface of PDMS film, indicating that the greater capacitance there is, the higher charge density might be obtained on it under same friction. To increase C_1 we could reduce d value while keep ϵ_1 unchanged. Reduction in the thickness of the pure PDMS film can only increase C_1 to some extent. However, from the investigations above, the increased output performance by mixing GPs into PDMS might be a result of equivalent reduction in the thickness of the PDMS film with a little change of its dielectric property. C_3 represents the capacitance of the PDMS mixed with GPs (Fig. 7b). From the conductivity measured in Fig. 3d and the relative dielectric constant in Table 1, we find that the relative dielectric constant has little change when the PDMS is mixed

with less than 0.1 g GPs. The capacitance C_3 is measured by two Al foil electrodes sandwiched with the PDMS film mixed with different GP contents as is shown in Table 1, from which we can see that C_3 reaches maximum with the GP content of 0.1 g. Too many GPs might cause the aggregation of them in the PDMS, which cannot provide a better enhancement of the capacitance. The maximum charge transfer quantity can be calculated from the current in a half cycle measured from the experiment which indicates the possible maximum charge quantity Q on the surface composite PDMS film. Then compared with the pure PDMS situation, Q/Q_0 is obtained as is shown in Table 1. The ratio of the effective thickness d of the PDMS film with different GP contents to that of pure PDMS film d/d_0 is calculated from the C/C_0 and ε_r . We can see that the d is most reduced for the PDMS film with GP content of 0.1 g, which matches the maximum charge Q in the same condition. The effective thickness d of dielectric film can decrease 34.68% and surface charges on the dielectric film can increase 111.27% for the PDMS film with GP content of 0.1 g.

To prove how the d value is reduced by mixing GPs in the PDMS film, we give more detailed discussion and draw schematic diagrams in Fig. 7b and c. As the carbon nanoparticles are uniformly distributed in the PDMS, they can be simply divided into layers, as is shown in Fig. 7b. Each carbon particle layer acts as a conductive panel. According to electromagnetics, the capacitance of a flat-panel capacitor with an inserted conductive panel (Fig. 7c) is $C = \frac{\varepsilon S}{d-r}$, where r is the thickness of the conductive panel, indicating that the thickness d reduces to $d-r$. Based on this principle, the sum of the every conductive layer is $\delta=r_1+r_2+\dots$ and the equivalent

capacitance of the capacitor separated by the PDMS@GPs film should be $C_3 = \frac{\epsilon_1 S}{d - \delta}$, proving the capacitance is greatly increased (Fig. 7d), which matches the enhanced output current due to the increase in charge density on the surface of the PDMS@GPs film suggested above. Though C_2 is not a fixed capacitor, its maximum energy storage also depends on the charge density on the electret friction film. Higher charge density produces larger energy storage and output. Here, we have a clearer understanding of the triboelectric generator with the capacitor structure which acts as an energy storage and output device. The ratio of the dielectric constant to the thickness of the polymer film directly determines the maximum charge density on the surface of electret polymer film, which further determines the maximum energy storage and output. The periodic mechanical force applied works as a pump to input electrical energy into the capacitor and drives the stored energy to external circuit based on the electrostatic induction effect. As for the cause of better performance of the PDMS mixed with the GPs than those of the graphene sheets and carbon fibers, the graphene sheets and fibers cannot be uniformly distributed in the PDMS film due to their morphologies, which easily destroys the dielectric property of the PDMS, as is shown in Table S1. Therefore, the dielectric property of the PDMS mixed with the GPs with sphere-like shape, size of 20-40 nm, 3.0 wt% content and thickness of 0.45 mm has a little change and presents a great enhancement of output power for the CFNG.

With an increase in the capacitance C_3 , the charge density on the surface of the PDMS@GPs film could be increased. Fig. 8a gives the output current of the CFNG

sandwiched with the PDMS@GPs film, from which we can see that the current increases within initial 7.5 s and afterward reaches a constant. This result indicates that the charge generated on the PDMS surface increases by the rubbing process and then achieves a maximum due to the limitation of the capacitance C_3 . In order to calculate the charge density on the surface of the PDMS film, we calculate the area below a half cycle of the current plot (Fig. S6c). The maximum charge transfer quantity is $Q_M=72.49$ nC in a half cycle, from which we can decide the charge density on the surface of PDMS film to be $181.23 \mu\text{C}/\text{m}^2$.

In order to demonstrate the integratability of the PDMS@GPs film, two CFNGs are fabricated and attached to the same hardboard. The output current of the two CFNGs (size: $1 \text{ cm} \times 2 \text{ cm}$) working in series and in parallel is given in Fig. 8b and the structure schematic diagram of the assembled two CFNGs (inset). The rectified output current of CFNG 1 and CFNG 2 with a small gap between the composite film and the electrodes is $5.22 \mu\text{A}$ and $4.15 \mu\text{A}$ (Fig. 8b) respectively at the oscillation frequency of 2 Hz. By connecting these two CFNGs in parallel, the output current increases to $9.23 \mu\text{A}$, which is approximately the sum of the current of each CFNG. When these two CFNGs are connected in series, the current output is $4.13 \mu\text{A}$ which has little change compared with the current ($4.15 \mu\text{A}$) of the individual CFNG. The results demonstrate a good integratability, indicating that the CFNG has a significant potential to be assembled into right size and given output device.

3. Experimental Section

Fabrication of PDMS@GPs Thin Films: Fig. 1a shows the schematic diagram of

the process in fabricating the PDMS@GPs thin film and CFNG device. In this experiment, the PDMS solution (Sylgard 184, Dow Corning) contains the elastomer (PDMS) and the curing agent. To achieve PDMS composite film, first, graphite particles (Sigma–Aldrich) dispersed in alcohol were mixed into PDMS by mechanical blender for 15 min (Elastomer was mixed thoroughly with the curing agent in the weight ratio of 10:1).³⁶ Secondly, the PDMS mixed with GPs was transferred to a cylindrical dish to form a thin film. Thirdly, the dish floating on the water in a beaker was put into a vacuum oven at 60 °C for 2.5 h. Then the PDMS@GPs thin films with different thicknesses (*i.e.* 0.15 mm, 0.30 mm, 0.45 mm, 0.60 mm, 0.75 mm) were made for comparative experiments. Finally, the composite film was assembled into a flexible CFNG device with Al foil electrodes and a piece of hardboard.

Fabrication of CFNGs: The CFNG has a sandwich structure with aluminum foil as the electrodes separated by the PDMS@GPs film. The bottom electrode was attached to the hardboard and the upper electrode was independent with a certain gap between the upper electrode and the surface of the composite film. Then, the device was placed in an oven at temperature of 60 °C to dry and the CFNG was fabricated after 5 min. The size of the gap was controlled by inserting the PET film with thickness of 0.1 mm in different numbers between the top electrode and the PDMS@GPs film (Fig. S7).

Characterization and Measurement of the CFNGs: The morphology and structure of the PDMS@GPs thin film was characterized by using a field emission scanning electron microscopy (Nova 400 Nano SEM). X-ray diffraction measurement (XRD) with Cu Ka radiation (wavelength is 1.5418 °Å) at a 2 degree/min scanning speed was

used to study the crystal phase. The CFNG was driven by an Electric Oscillator (JZK-5) controlled by Function Signal Generator/Counter (NDY-EE1641D) and a Power Amplifier (YE5871A). The output signals of CFNG were put into a Stanford low-noise current Preamplifier (Model SR570) to filter noise signals, and then were collected and analyzed by the Data Acquisition Card (NI PCI-6259) on the Desktop PC (Fig. S8). The conductivity, relative dielectric constant and capacitance of the PDMS film were characterized by the Broadband Dielectric Spectrometer (Germany NOVOCONTROL Concept 40).

4. Conclusion

In summary, the PDMS-based composite film nanogenerators (CFNG) by mixing PDMS with graphite particles (GPs) have been fabricated. Their output current, voltage and power are investigated systematically by mixing GPs in different particle sizes and contents, and by varying the CFNG structure with different film thicknesses and gaps between the electrode and composite film, under different conditions. The most significant finding in this work is that the working mechanism of CFNG is proposed in details and a clearer understanding of triboelectric generator with capacitor structure is presented. The findings suggest the generator both act as an energy storage and energy output device. The ratio of the dielectric constant to thickness (ϵ/d) of the polymer film directly decides the maximum charge density on the surface of the electret polymer film, and further determines the maximum energy storage and output. The periodic mechanical force applied works as a pump to put electrical energy into the capacitor and to drive the stored energy to external circuit based on the electrostatic induction

effect. Bigger ϵ/d value achieves higher charge density on the polymer surface and contributes to a larger output power of the CFNG. The effective d value can be largely reduced by mixing PDMS with a suitable amount of conductive carbon nanoparticles with a little change of its dielectric property. This finding can be applied to all the triboelectric NGs with capacitor structure and provide an important guide to the structure design for NGs. The GPs with size of 20-40 nm and 3.0% mass percentage mixed into the PDMS can reduce 34.68% of the effective thickness of dielectric film and increase 111.27% of the surface charges on the dielectric film. The output power of the CFNG is 1.48 mW (3.7 W/m^2) has been obtained and used to light up at least 52 blue LEDs in series. The CFNG has good time stability, durability and integratability. With advantages of high output power and biocompatible properties, the CFNG has wide application prospects in flexible sensors and biological devices field.

Acknowledgements

This work is supported by the NSFCQ (cstc2012jjB0006), the National High Technology Research and Development Program of China (SQ2015AA0302342), SRFDP (20110191110034, 20120191120039), NSFC (11204388), the Fundamental Research Funds for the Central Universities (CDJRC10300001, CDJZR11300004, CDJZR12225501, CQDXWL-2013-012).

Supporting Information Available at <http://pubs.acs.org>.

References

- 1 Z. L. Wang and J. H. Song, *Science*, 2006, **312**, 242-246.
- 2 X. D. Wang, J. H. Song, J. Liu and Z. L. Wang, *Science*, 2007, **316**, 102-105.

- 3 W. Z. Wu, C. F. Pan, Y. Zhang, X. N. Wen and Z. L. Wang, *Nano Today*, 2013, **8**, 619-642.
- 4 M. D. Han, X. S. Zhang, B. Meng, W. Liu, W. Tang, X. M. Sun, W. Wang and H. X. Zhang, *ACS Nano*, 2013, **7**, 8554-8560.
- 5 M. P. Lu, J. Song, M. Y. Lu, M. T. Chen, Y. Gao, L. J. Chen and Z. L. Wang, *Nano lett.*, 2009, **9**, 1223-1227.
- 6 Y. Yang, J. H. Jung, B. K. Yun, F. Zhang, K. C. Pradel, W. X. Guo and Z. L. Wang, *Adv. Mater.*, 2012, **24**, 5357-5362.
- 7 Y. Yang, W. X. Guo, K. C. Pradel, G. Zhu, Y. S. Zhou, Y. Zhang, Y. F. Hu, L. Lin and Z. L. Wang, *Nano lett.*, 2012, **12**, 2833-2838.
- 8 F. R. Fan, L. Lin, G. Zhu, W. Z. Wu, R. Zhang and Z. L. Wang, *Nano lett.*, 2012, **12**, 3109-3114.
- 9 S. H. Wang, L. Lin, Y. N. Xie, Q. S. Jing, S. M. Niu and Z. L. Wang, *Nano lett.*, 2013, **13**, 2226-2233.
- 10 S. H. Wang, Y. N. Xie, S. M. Niu, L. Lin and Z. L. Wang, *Adv. Mater.*, 2014, **26**, 2818-2824.
- 11 J. W. Zhong, Q. Z. Zhong, F. R. Fan, Y. Zhang, S. H. Wang, B. Hu and Z. L. Wang, J. Zhou, *Nano Energy*, 2013, **2**, 491-497.
- 12 L. Lin, S. H. Wang, Y. N. Xie, Q. S. Jing, S. M. Niu, Y. F. Hu and Z. L. Wang, *Nano lett.*, 2013, **13**, 2916-2923.
- 13 G. Zhu, J. Chen, Y. Liu, P. Bai, Y. S. Zhou, Q. S. Jing, C. F. Pan and Z. L. Wang, *Nano lett.*, 2013, **13**, 2282-2289.

- 14 H. Y. Guo, X. M. He, J. W. Zhong, Q. Zhong, Q. Leng, C. G. Hu, J. Chen, L. Tian, Y. Xi and J. Zhou, *J. Mater. Chem. A*, 2014, **2**, 2079-2087.
- 15 R. H. Que, M. W. Shao, S. D. Wang, D. D. D. Ma and S. T. Lee, *Nano lett.*, 2011, **11**, 4870-4873.
- 16 R. H. Que, Q. Shao, Q. L. Li, M. W. Shao, S. D. Cai, S. D. Wang and S. T. Lee, *Angew. Chem. Int. Edit.*, 2012, **51**, 5418-5422.
- 17 Z. H. Lin, Y. Yang, J. M. Wu, Y. Liu, F. Zhang and Z. L. Wang, *J. Phys. Chem. Lett.*, 2012, **3**, 3599-3604.
- 18 G. A. Zhu, R. S. Yang, S. H. Wang and Z. L. Wang, *Nano lett.*, 2010, **10**, 3151-3155.
- 19 B. Bhushan, D. Hansford and K. K. Lee, *J. Vac. Sci. Technol. A*, 2006, **24**, 1197-1202.
- 20 S. C. B. Mannsfeld, B. C. K. Tee, R. M. Stoltenberg, C. Chen, S. Barman, B. V. O. Muir, A. N. Sokolov, C. Reese and Z. N. Bao, *Nat. Mater.*, 2010, **9**, 859-864.
- 21 Y. Yang, H. L. Zhang, J. Chen, S. M. Lee, T. C. Hou and Z. L. Wang, *Energ. Environ. Sci.*, 2013, **6**, 1744-1749.
- 22 K. I. Park, M. Lee, Y. Liu, S. Moon, G. T. Hwang, G. Zhu, J. E. Kim, S. O. Kim, D. K. Kim, Z. L. Wang and K. J. Lee, *Adv. Mater.*, 2012, **24**, 2999-3004.
- 23 H. Sun, H. Tian, Y. Yang, D. Xie, Y. C. Zhang, X. Liu, S. Ma, H. M. Zhao and T. L. Ren, *Nanoscale*, 2013, **5**, 6117-6123.
- 24 J. J. Wang, T. H. Hsu, C. N. Yeh, J. W. Tsai and Y. C. Su, *J. Micromech. Microeng.*, 2012, **22**, 015013.

- 25 H. I. Lin, D. S. Wu, K. C. Shen and R. H. Horng, *ECS J. Solid State Sci. Technol.*, 2013, **2**, P400-P404.
- 26 K. I. Park, S. B. Bae, S. H. Yang, H. I. Lee, K. Lee and S. J. Lee, *Nanoscale*, 2014, **6**, 8962-8968.
- 27 Y. C. Mao, P. Zhao, G. McConohy, H. Yang, Y. X. Tong and X. D. Wang, *Adv. Energy Mater.*, 2014, **4**, 1301624.
- 28 K. Y. Lee, J. Chun, J.-H. Lee, K. N. Kim, N.-R. Kang, J.-Y. Kim, M. H. Kim, K.-S. Shin, M. K. Gupta, J. M. Baik and S.-W. Kim, *Adv. Mater.*, 2014, **26**, 5037-5042.
- 29 G. Cheng, Z. H. Lin, Z. L. Du and Z. L. Wang, *ACS Nano*, 2014, **8**, 1932-1939.
- 30 W. Tang, B. Meng and H. X. Zhang, *Nano Energy*, 2013, **2**, 1164-1171.
- 31 Y. N. Xie, S. H. Wang, L. Lin, Q. S. Jing, Z. H. Lin, S. M. Niu, Z. Y. Wu and Z. L. Wang, *ACS Nano*, 2013, **7**, 7119-7125.
- 32 P. Bai, G. Zhu, Z. H. Lin, Q. S. Jing, J. Chen, G. Zhang, J. Ma and Z. L. Wang, *ACS Nano*, 2013, **7**, 3713-3719.
- 33 Y. H. Ko, G. Nagaraju, S. H. Lee and J. S. Yu, *ACS Appl. Mater. Inter.*, 2014, **6**, 6631-6637.
- 34 J. Chen, G. Zhu, W. Q. Yang, Q. S. Jing, P. Bai, Y. Yang, T. C. Hou and Z. L. Wang, *Adv. Mater.*, 2013, **25**, 6094-6099.
- 35 G. Zhu, J. Chen, T. J. Zhang, Q. S. Jing and Z. L. Wang, *Nat. Commun.*, 2014, **5**, 3426-3435.

36 P. Yi, R. A. Awang, W. S. T. Rowe, K. Kalantar-zadeh and K. Khoshmanesh,

Lab Chip, 2014, **14**, 3419-3426.

Table 1. The measured relative dielectric constant (ϵ_r) of the PDMS@GPs films, the measured capacitance C_3 , calculated charge change (Q/Q_0) from the output voltage and effective thickness change (d/d_0) calculated by the capacitance change (C/C_0) of the CFNG with different GP contents.

GPs (g)	0.000	0.005	0.010	0.030	0.050	0.080	0.100	0.200	0.300	1.000
ϵ_r	3.000	2.999	2.995	2.989	2.987	2.980	2.973	2.629	2.162	0.637
C_3 (pF)	23.11	--	25.73	--	30.22	33.63	35.85	26.81	22.01	--
Q/Q_0	1.000	--	1.272	--	1.656	1.906	2.113	1.387	0.975	--
d/d_0	1.000	--	0.917	--	0.778	0.698	0.653	0.772	0.775	--

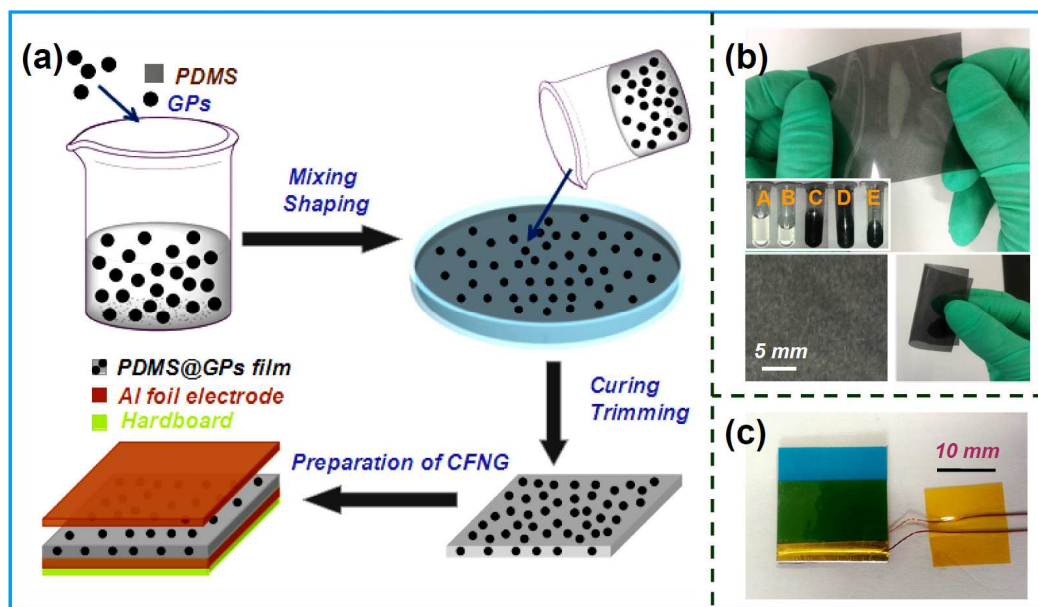


Fig. 1. (a) Schematic diagram of process for fabricating the PDMS@GPs thin film and CFNG. (b) The digital photograph of the flexible PDMS@GPs thin film. The materials in centrifuge tubes in the inset from A to E are pure PDMS, pure curing agent, GPs dispersed in alcohol, PDMS@GPs mixed in alcohol, curing agent@GPs dispersed in alcohol, respectively. (c) The digital photograph of the CFNG device.

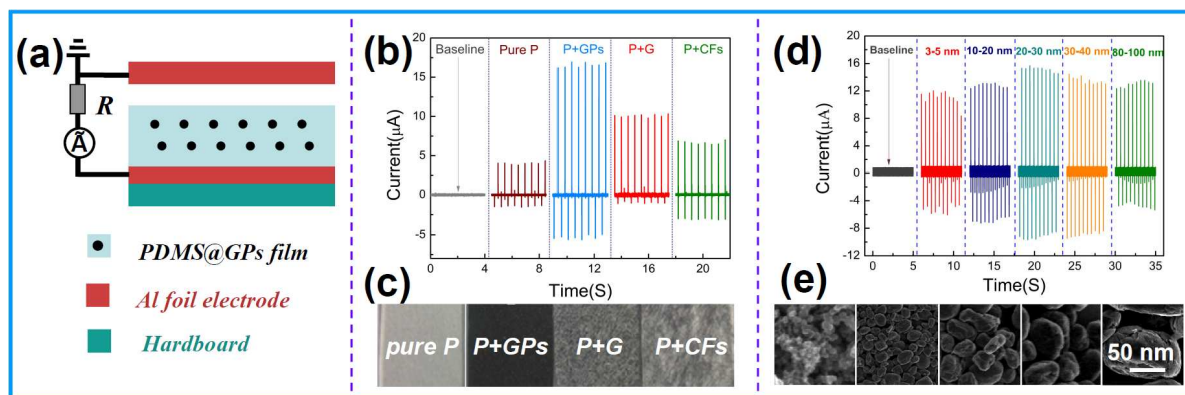


Fig. 2. The schematic diagram of CFNG's cross section (a). The out put current (b) and photographs (c) of the CFNG using the pure PDMS film (Pure P), and PDMS film mixed with graphite particles (P+GPs), graphenes (P+G) and carbon fibers (P+CFs). The output current (d) and FE-SEM images (e) of the CFNG using the composite film with different sizes of GP.

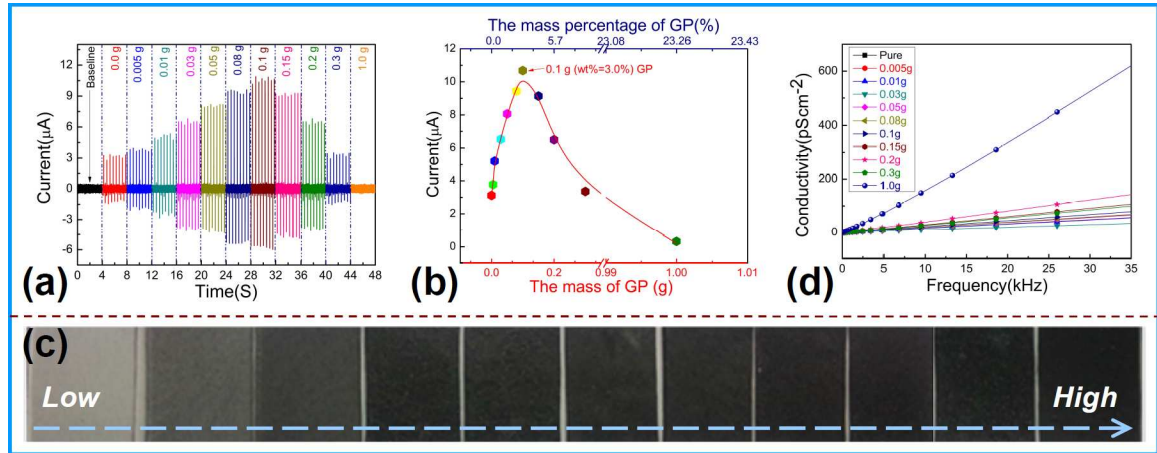


Fig. 3. The output current of CFNGs using the composite film with different GP weights (a) and mass percentages (b) in the same film size (2 cm \times 2 cm) and thickness (0.45 mm), measured at the frequency of 2 Hz. The conductivities (c) and digital photographs (d) of the PDMS@GPs film with GP content from 0.0 g to 1.0 g.

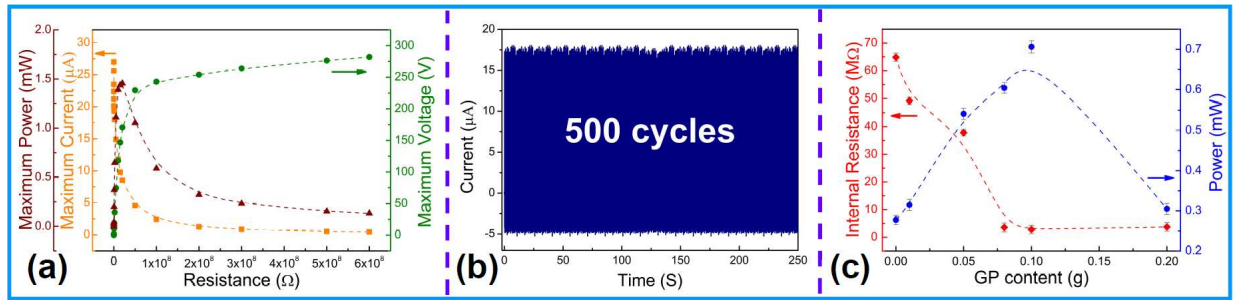


Fig. 4. (a) The maximum output voltage, current and power under different external loads. (b) The stability and durability test of CFNG under 500 cycles. (c) The plots of the internal resistance and the output power of the devices versus different GP contents in PDMS film.

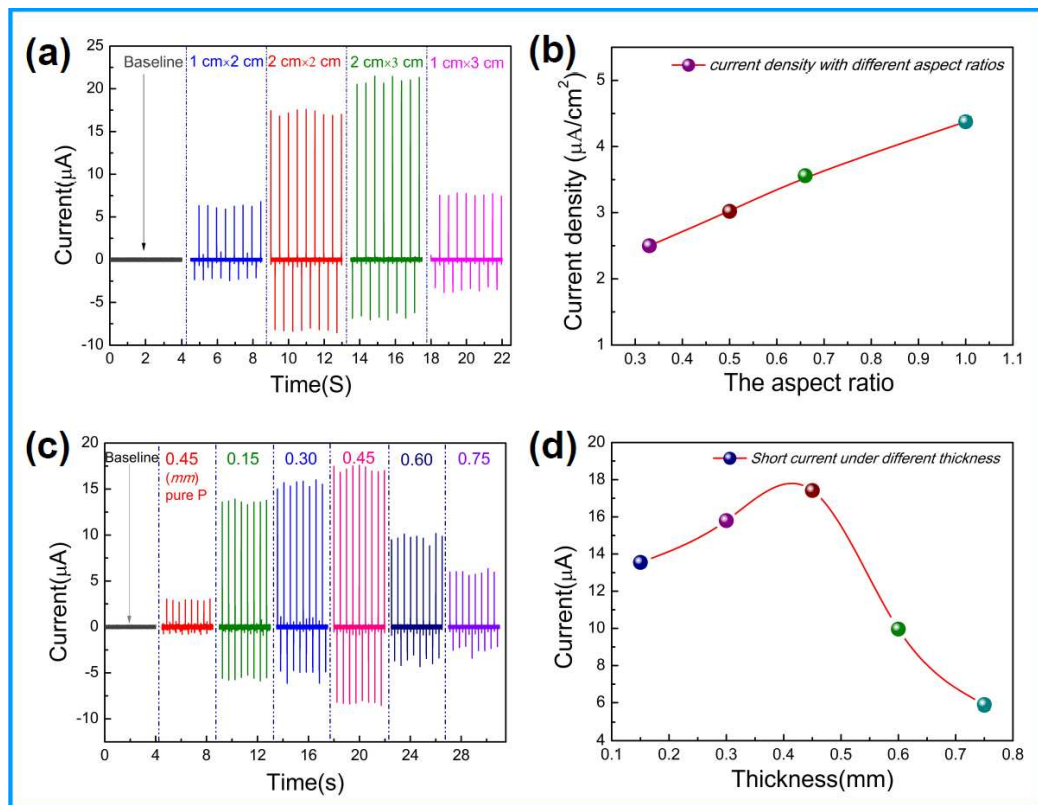


Fig. 5. The output current (a) and current density (b) of the CFNG using the PDMS@GPs film (0.1 g GPs) with different aspect ratios (a-b) and with different thicknesses (c-d).

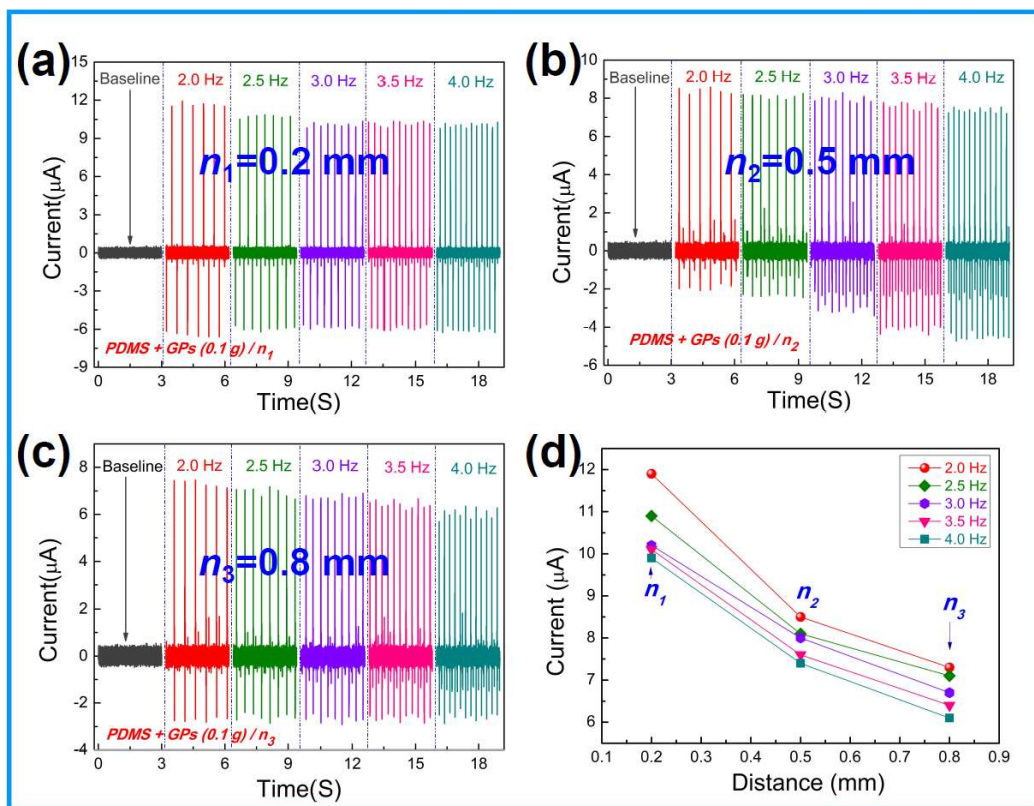


Fig. 6. The CFNG with different gaps (n) between the upper electrode and the composite film, 0.2 mm (a), 0.5 mm (b), 0.8 mm (c) under different driving frequencies $f=2.0, 2.5, 3.0, 3.5, 4.0$ Hz. The plots of the output current versus the gap under different driving frequencies (d).

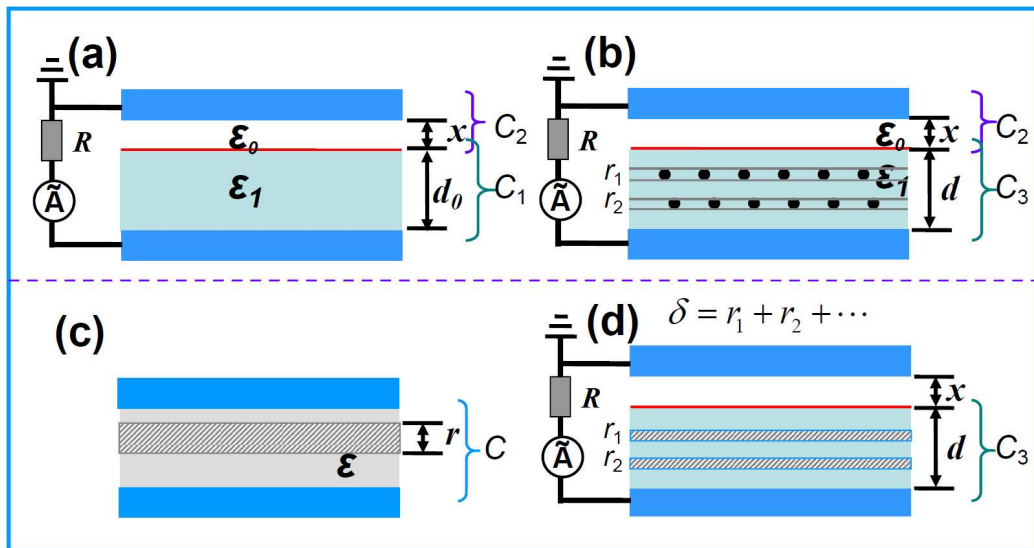


Fig. 7. The schematic diagram of CFNG's cross section and its capacitor structure separated by pure PDMS film (a) and PDMS@GPs thin film (b). A capacitor with conductive panel (thickness r) inserted in the dielectric film (c) and the equivalent capacitance of the CFNG separated by PDMS@GPs thin film (d).

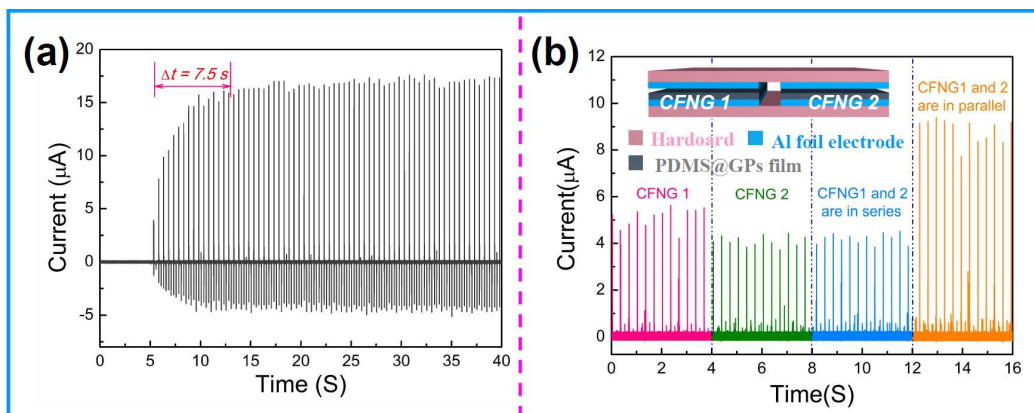


Fig. 8. (a) The output current of the CFNG sandwiched with the PDMS@GPs film working in initial 7.5 s. (b) Current output measured from CFNG 1 and 2 (the same size: $2\text{ cm} \times 1\text{ cm}$) when they are connected in series and in parallel after rectified at the applied oscillation frequency of 2 Hz, the inset is the assembly method diagram.